NNLO QCD corrections to *t*-channel single top quark production and decay

Edmond L. Berger,[1,*] Jun Gao,[1,2,†] C.-P. Yuan,[3,‡] and Hua Xing Zhu[4,§]

[1]*High Energy Physics Division, Argonne National Laboratory (ANL), Argonne, Illinois 60439, USA*
[2]*Kavli Institute for Theoretical Physics, University of California, Santa Barbara, California 93106, USA*
[3]*Department of Physics and Astronomy, Michigan State University, East Lansing, Michigan 48824, USA*
[4]*Center for Theoretical Physics, Massachusetts Institute of Technology,*
Cambridge, Massachusetts 02139, USA

We present a fully differential next-to-next-to-leading-order calculation of *t*-channel single top quark production and decay at the LHC under a narrow-width approximation and neglecting cross talk between incoming protons. We focus on the fiducial cross sections at 13 TeV, finding that the next-to-next-to-leading-order QCD corrections can reach the level of -6%. The scale variations are reduced to the level of a percent. Our results can be used to improve experimental acceptance estimates and the measurements of the single top quark production cross section and the top quark electroweak couplings.

I. INTRODUCTION

The top quark can be produced singly at a hadron collider through the electroweak Wtb vertex. There are three production channels: the *t*-channel and *s*-channel processes through exchange of a W boson and associated production of tW. All three channels are sensitive to the structure of the Wtb vertex and to the Cabibbo-Kobayashi-Maskawa matrix element V_{tb}, an important motivation for their study. Moreover, single top production provides an important window to physics beyond the standard model (SM) [1], e.g., a modified Wtb vertex, new heavy quarks, new gauge bosons, flavor-changing neutral current, and so forth. Single top quark production was first established at the Fermilab Tevatron [2,3] and later at the Large Hadron Collider (LHC) [4–7]. Single top quark studies are expected to enter an era of high precision during the upcoming run of the LHC at higher energy and larger luminosity.

The *t*-channel production has the largest rate among the three at the LHC, about 210 pb at $\sqrt{s} = 13$ TeV. Significant efforts to improve the theoretical description of this process include next-to-leading-order (NLO) QCD corrections in both four- and five-flavor schemes in Refs. [8–16]. Soft gluon resummation has been considered in Refs. [17–20]. Matching NLO calculations to parton showers is done in Refs. [21–23]. Recently, next-to-next-to-leading-order (NNLO) QCD corrections with a *stable* top quark were calculated in Ref. [24], neglecting certain subleading contributions in color.

In this manuscript we present the first fully differential NNLO calculation of *t*-channel single top quark *production and decay* at the LHC in the five-flavor scheme in QCD.

We follow Ref. [24] in neglecting cross talk between the hadronic systems of the two incoming protons. To the best of our knowledge, our calculation is the first to combine QCD corrections at NNLO for production and decay, meaning that a realistic simulation at NNLO is now available for leptonic top quark decay in *t*-channel single top quark production. The differential nature of our calculation allows us to impose phase-space selections on final state objects, as done in the experiments (fiducial cuts). Using the fiducial cuts of the ATLAS and CMS analyses [25,26], we find large NLO corrections, thus necessitating the higher-order calculation performed here. The uncertainties associated with QCD hard-scale variation are reduced to the level of $\sim 1\%$. We compute the ratio of the top antiquark to top quark production distributions with fiducial cuts applied, showing that sensitivity of this charge ratio to current parton distribution functions is much larger than to the perturbative corrections.

In the remaining paragraphs we outline the methods used in the calculation, and we present our numerical results on inclusive cross sections and fiducial cross sections and various differential distributions.

II. METHOD

We work in the narrow-width approximation (NWA), under which the QCD corrections to the top quark production and decay are factorizable. As confirmed by explicit numerical studies of off-shell and nonfactorizable corrections [27,28], this approximation is justified because the top quark decay width is much smaller than its mass. We approximate the full QCD corrections by the *vertex* corrections; in the inclusive case, this is known as the structure function approach [29]. In this approach, we separate the QCD corrections into three factorizable contributions, as sketched in Fig. 1. There is a decay part V_d; the light-quark line of the production part V_l; and the
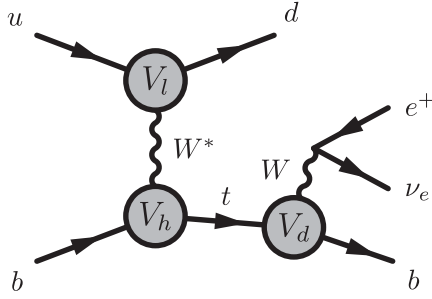
*[*]berger@anl.gov
[†]jgao@anl.gov
[‡]yuan@pa.msu.edu
[§]zhuhx@mit.edu

FIG. 1. Sketch of t-channel single top quark production and decay; $ub \to dt$ with $t \to e^+\nu_e b$. V_l represents QCD corrections to the light-quark line, which could include interference of the tree diagram and the two-loop diagram, square of the one-loop diagram (double-virtual), interference of the one-loop diagram with one additional gluon and the tree-level diagram with one additional gluon (real-virtual), and the square of tree-level diagram with a pair of additional partons (double-real). V_h and V_d represent the same type of corrections to the heavy-quark line and the decay part, respectively. There is no cross talk between the light-quark line, heavy-quark line, and the decay part in our calculation.

heavy-quark line of the production part V_h. The use of the (fully differential) structure function approximation builds on the observation that QCD interference between the light-quark line and the heavy-quark line vanishes at NLO and is suppressed at least by a factor of $1/N_c^2$ at NNLO. The use of such an approximation is also crucial for making this calculation feasible, because interference contributions between the light- and heavy-quark lines are not yet available [30] for the full two-loop virtual diagrams. The structure function approximation at NNLO is also used in an earlier calculation of t-channel on-shell single top quark production [24] and in Higgs boson production through weak boson fusion [31,32].

The NNLO QCD corrections to the heavy-quark line are straightforward if we use phase-space slicing with the N-jettiness variable [33–35]. A similar calculation was performed for charm quark production in neutrino deep inelastic scattering (DIS) in Ref. [36]. For the corrections to the light-quark line, we adopted the method of "projection-to-Born" in Ref. [32]. The key ingredients in this approach are the inclusive NNLO DIS coefficient functions [37–39], for which a conveniently parametrized version is available [40,41]. For the real-virtual corrections, we extracted the one-loop helicity amplitudes from DIS two-jet production in Ref. [42], and we cross-checked with Gosam [43]. These ingredients were combined according to Ref. [32], by constructing appropriate counterevents with opposite weights for every event in the Monte Carlo (MC) integration of double-real and real-virtual contributions, which render the phase-space integrals finite for infrared (IR) safe observables. For the decay part of the calculation, we adopted the results in Ref. [44]. We also take into account the product of two NLO corrections from different

combinations of the light-quark line, the heavy-quark line, and the decay part.

Finally, we combine corrections to the production part and decay part consistently in the NWA, as in Refs. [45–47]. Schematically, we write

$$\sigma^{\text{LO}} = \frac{1}{\Gamma_t^0} d\sigma^0 d\Gamma_t^0,$$

$$\delta\sigma^{\text{NLO}} = \frac{1}{\Gamma_t^0}\left[d\sigma^1 d\Gamma_t^0 + d\sigma^0\left(d\Gamma_t^1 - \frac{\Gamma_t^1}{\Gamma_t^0}d\Gamma_t^0\right)\right],$$

$$\delta\sigma^{\text{NNLO}} = \frac{1}{\Gamma_t^0}\left[d\sigma^2 d\Gamma_t^0 + d\sigma^1\left(d\Gamma_t^1 - \frac{\Gamma_t^1}{\Gamma_t^0}d\Gamma_t^0\right)\right.$$
$$\left. + d\sigma^0\left(d\Gamma_t^2 - \frac{\Gamma_t^2}{\Gamma_t^0}d\Gamma_t^0 - \frac{\Gamma_t^1}{\Gamma_t^0}\left(d\Gamma_t^1 - \frac{\Gamma_t^1}{\Gamma_t^0}d\Gamma_t^0\right)\right)\right],$$
$$(1)$$

where $d\sigma^i$ and $d\Gamma_t^i$ denote the $\mathcal{O}(\alpha_S^i)$ corrections to the production and decay parts, respectively. For the full NNLO corrections there are contributions from $\mathcal{O}(\alpha_S^2)$ production only, from the product of $\mathcal{O}(\alpha_S)$ production and $\mathcal{O}(\alpha_S)$ decay, and from $\mathcal{O}(\alpha_S^2)$ decay only, as shown in Eq. (1). Inclusive production cross sections at each order can be obtained after integration over the decay phase space.

III. NUMERICAL RESULTS

We use a top quark mass of 173.2 GeV and a W boson mass of 80.385 GeV. We set the W boson decay branching ratio to 0.1086 for one lepton family. We choose $|V_{tb}| = 1$ and the CT14 NNLO parton distribution functions (PDFs) [48] with $\alpha_s(M_Z) = 0.118$. The nominal central scale choice is $\mu_R = \mu_F = m_t$ with scale variation calculated by varying the two together over the range $0.5 < \mu/\mu_o < 2$. We list the LO, NLO and NNLO results for top quark and antiquark production in Table I. The NNLO QCD corrections reduce the cross sections by 2%–3% compared to a reduction of 4%–5% at NLO. The full NNLO corrections consist of pieces from the heavy-quark line, the light-quark line, and the products of them. There are cancellations between these pieces as well as cancellations among different partonic channels. Perturbative convergence of the separate QCD series is well maintained, as we verified by checking the individual pieces. Variations of the

TABLE I. Inclusive cross sections for top (anti)quark production at 13 TeV at various orders in QCD. The scale uncertainties are calculated by varying the hard scale from $\mu_F = \mu_R = m_t/2$ to $2m_t$ and are shown in percentages.

Inclusive [pb]	LO	NLO	NNLO
t quark	$143.7^{+8.1\%}_{-10\%}$	$138.0^{+2.9\%}_{-1.7\%}$	$134.3^{+1.0\%}_{-0.5\%}$
$\bar{t}$ quark	$85.8^{+8.3\%}_{-10\%}$	$81.8^{+3.0\%}_{-1.6\%}$	$79.3^{+1.0\%}_{-0.6\%}$

theoretical results associated with choices of the hard scales are reduced by a factor of 4 at NLO compared with LO and by a further factor of 3 at NNLO with respect to NLO.

Fiducial cross sections for t-channel single top quark production have been measured at 7 and 8 TeV [25,26]. We choose a fiducial region for 13 TeV that is similar to the one used in the CMS analysis [26] at 8 TeV. We use the anti-k_T jet algorithm [49] with a distance parameter $D = 0.5$. Jets are defined to have transverse momentum $p_T > 40$ GeV and pseudorapidity $|\eta| < 5$. We require exactly two jets in the final state, following the CMS and ATLAS analyses, meaning that events with additional jets are vetoed, and we require at least one of these to be a b jet with $|\eta| < 2.4$ [50,51]. We demand the charged lepton to have a p_T greater than 30 GeV and rapidity $|\eta| < 2.4$. For the fiducial cross sections reported below we include top quark decay to only one family of leptons.

Table II shows our predictions of the fiducial cross sections at different perturbative orders, with scale variations shown in percentages. We vary the renormalization and factorization scales $\mu_R = \mu_F$ in the top quark production stage, and the renormalization scale in the decay stage, independently by a factor of 2 around the nominal scale choice. The resulting scale variations are added in quadrature to obtain the numbers shown in Table II. We also show the QCD corrections from production and decay separately as defined in Eq. (1). All results shown in Table II are for the central scale choice m_t, as for the inclusive cross sections. The NNLO corrections from the product of $\mathcal{O}(\alpha_S)$ production and $\mathcal{O}(\alpha_S)$ decay can be derived by subtracting the above two contributions from the full NNLO corrections.

Changes of the QCD corrections after all kinematic cuts are applied are evident if one compares Table II with Table I. Acceptance in the charged lepton, the b jet, and the non-b jet produce these changes, as well as the jet veto. We call attention to the fact that the NLO QCD corrections in production have changed to -19%. The NLO corrections in decay further reduce the cross sections by about 8%. At NNLO the correction in production

is still dominant and can reach -6%. The size of the NNLO correction in decay is smaller by about a factor of 2, and it almost cancels with the correction from the product of one-loop production and one-loop decay. Scale variations have been reduced to about $\pm 1\%$ at NNLO. Scale variation bands at various orders do not overlap with each other in general.

With fiducial cuts applied, the jet veto introduces another hard scattering scale of $p_{T,\mathrm{veto}} = 40$ GeV in addition to m_t. Thus it may be appropriate to choose a QCD scale of $(p_{T,\mathrm{veto}} m_t)^{1/2} \sim m_t/2$, especially at lower perturbative orders where the gluon splitting contributions are absorbed into the bottom quark PDF. Alternative results with a central scale choice of $m_t/2$ in production, with the central scale m_t retained in the decay part, show better convergence of the series although the NNLO predictions are almost unchanged.

In experimental analyses, the total inclusive cross sections are usually determined through extrapolation of the fiducial cross sections based on acceptance estimates obtained from MC simulations. We can use the numbers shown in Tables I and II to derive the parton-level acceptance at various orders. For top quark production, the acceptances are 0.0283, 0.0214, and 0.0201 at LO, NLO, and NNLO, respectively. The NNLO corrections can change the acceptance by 6% relative to the NLO value. This change also propagates into the measurement of the total inclusive cross section through extrapolation.

To compare our results with those in Ref. [24], we calculated the NNLO total inclusive cross sections at 8 TeV using the same choices of parameters. We found a difference of $\sim 1\%$ on the NNLO cross sections. With a refined comparison through private communications, we traced the source of this discrepancy to NNLO contributions associated with V_h, with the b-quark initial state. All other parts in the NNLO corrections and all parts of the NLO contributions agree between the two results within numerical uncertainties. It has not been possible to further pin down the differences. We leave this issue for possible future investigation.

TABLE II. Fiducial cross sections for top (anti)quark production with decay at 13 TeV at various orders in QCD with a central scale choice of m_t in both production and decay. The scale uncertainties correspond to a quadratic sum of variations from scales in production and decay and are shown in percentages. Corrections from pure production and decay are also shown.

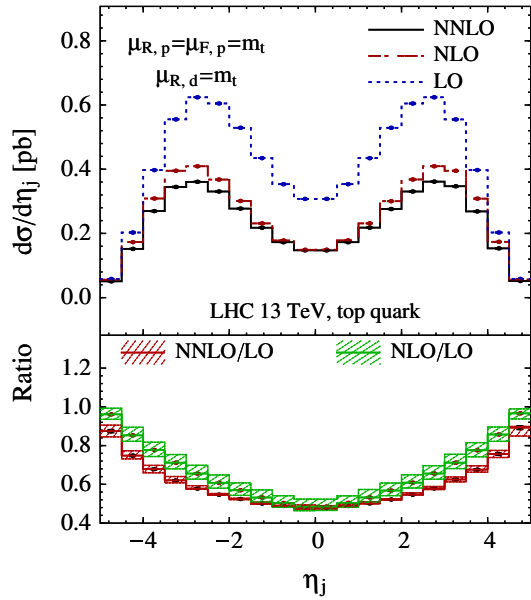| Fiducial [pb]		LO	NLO	NNLO
	Total	$4.07^{+7.6\%}_{-9.8\%}$	$2.95^{+4.1\%}_{-2.2\%}$	$2.70^{+1.2\%}_{-0.7\%}$
t quark	Corrections in production		-0.79	-0.24
	Corrections in decay		-0.33	-0.13
	Total	$2.45^{+7.8\%}_{-10\%}$	$1.78^{+3.9\%}_{-2.0\%}$	$1.62^{+1.2\%}_{-0.8\%}$
$\bar{t}$ quark	Corrections in production		-0.46	-0.15
	Corrections in decay		-0.21	-0.08

FIG. 2. Predicted pseudorapidity distribution of the non-b jet in the final state from top quark production with decay at 13 TeV with fiducial cuts applied.

IV. DIFFERENTIAL DISTRIBUTIONS

We present differential distributions including NNLO corrections for top quark production with decay. The effects for top antiquark distributions are similar. The full QCD corrections for the pseudorapidity distribution of the non-b jet are shown in Fig. 2 after all fiducial cuts are applied. Events with two b jets in the fiducial region are not
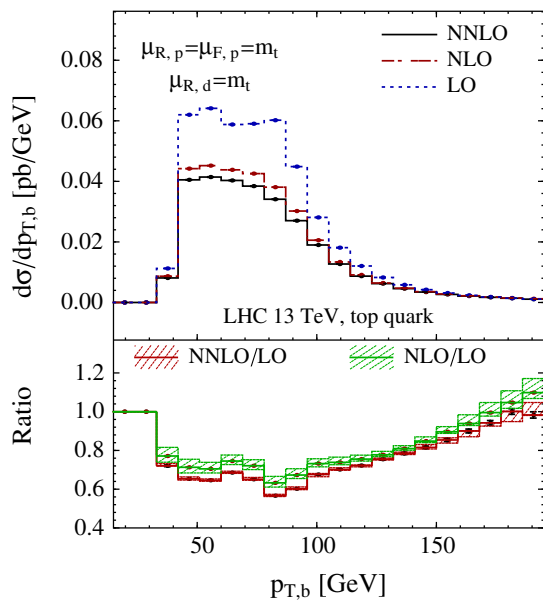
included in the plot. The corrections depend strongly on the pseudorapidity. The NNLO corrections have a different shape from those at NLO and can be even larger than the NLO corrections in the regions of large pseudorapidity. The transverse momentum distribution of the leading b jet is plotted in Fig. 3, again including the full QCD corrections in production and decay. The corrections reach a maximum for $p_{T,b}$ of about 80 GeV. Acceptance limitations explain the peculiar shape of the p_T distribution. We observe a reduction in the hard scale variations in both Figs. 2 and 3, calculated by varying the corresponding scales in production and decay independently by a factor of 2 around m_t and then adding the variations in quadrature. In general we found large NLO corrections to the fiducial distributions, which makes our NNLO calculation a necessity in order to assess the convergence and reliability of pQCD series.

As mentioned in Sec. II, we neglect cross talk between incoming protons, and we discuss the justification for this approximation for the inclusive cross section. Exchanges associated with cross talk, although suppressed by a factor of $1/N_c^2$, might lead to different kinematical shape dependence for differential distributions, compared with the corrections considered in this manuscript. It would be valuable to compute the cross-talk contributions in the future, once the relevant techniques are developed. We believe that the calculation presented in this manuscript represents the best available results in the literature so far.

Charge asymmetry is one of the precision observables at the LHC, e.g., as measured in W boson production

FIG. 3. Predicted transverse momentum distribution of the leading b jet from top quark production with decay at 13 TeV with fiducial cuts applied.
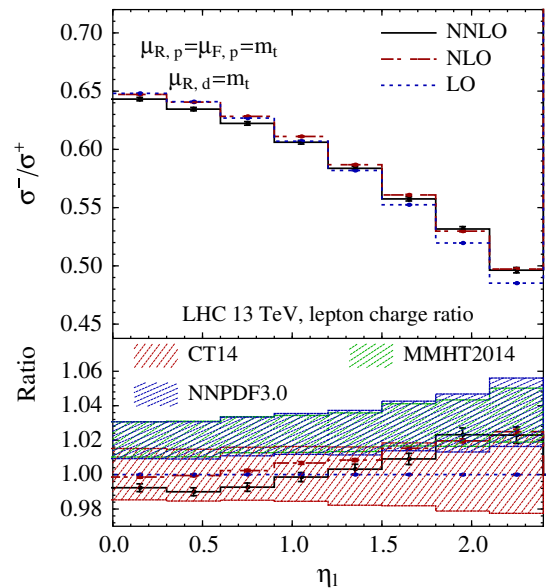

FIG. 4. Ratios of the fiducial cross sections of top antiquark to top quark production with decay at 13 TeV as a function of the pseudorapidity of the charged lepton. The lower panel shows ratios to the LO prediction as well as dependence on the choice of PDFs.

[52–54]. It is insensitive to high-order corrections and is less subject to experimental systematic uncertainties. Moreover, since it is determined largely by the PDFs, it can provide stringent constraints in PDF determinations [48,55]. The predicted ratio of the fiducial cross sections for top antiquark and top quark production is presented in the upper panel of Fig. 4 as a function of the pseudorapidity of the charged lepton. The ratio is less than one since there are more *u*-valence quarks than *d*-valence quarks in the proton, and it decreases with pseudorapidity because the d/u ratio decreases at large x [48]. The uncertainty flags show the statistical uncertainty from the MC integration. The ratios of the three curves are shown in the lower panel. The spread of the LO, NLO, and NNLO predictions is about 1% in the central region. At large $|\eta_l|$, the NLO correction can reach about 2%, and the additional NNLO correction is well below one percent. Also shown in the lower panel are the 68% confidence-level uncertainty bands for three sets of NNLO PDFs: CT14 [48], MMHT2014 [56] and NNPDF3.0 [57]. For simplicity, we obtained these bands using the LO matrix elements and the NNLO PDFs, and we verified that quantitatively similar central values of the bands are obtained if we use NLO matrix elements. Since the PDF-induced uncertainty is much larger than the theoretical uncertainty of its NNLO prediction, the charge ratio can be used reliably to further discriminate among and constrain the PDFs, provided that experimental uncertainties can be controlled to the same level, as is also pointed out in [24,58,59]. This charge ratio may also be sensitive to certain kinds of physics beyond the SM [60].

V. SUMMARY

We present the first calculation of NNLO QCD corrections to *t*-channel single top quark production with decay at the LHC in the five-flavor scheme in QCD, neglecting the cross talk between the hadronic systems of the two incoming protons. Our calculation provides a fully differential simulation at NNLO for *t*-channel single top quark production with leptonic decay at the parton level. The NNLO corrections reduce the scale uncertainties of the theoretical predictions to a percent level. For the kinematic cuts used in the 8 TeV LHC experimental analyses, the NNLO corrections to the fiducial cross sections can reach −6%. Our results can be used to improve the determinations of the single top quark production cross section and the top quark electroweak coupling.

ACKNOWLEDGMENTS

[1] T. M. P. Tait and C. P. Yuan, Phys. Rev. D **63**, 014018 (2000).
[2] T. Aaltonen *et al.* (CDF Collaboration), Phys. Rev. Lett. **103**, 092002 (2009).
[3] V. M. Abazov *et al.* (D0 Collaboration), Phys. Rev. Lett. **103**, 092001 (2009).
[4] ATLAS Collaboration, Phys. Lett. B **717**, 330 (2012).
[5] ATLAS Collaboration, Phys. Lett. B **716**, 142 (2012).
[6] CMS Collaboration, J. High Energy Phys. 12 (2012) 035.
[7] CMS Collaboration, Phys. Rev. Lett. **110**, 022003 (2013).
[8] G. Bordes and B. van Eijk, Nucl. Phys. **B435**, 23 (1995).
[9] R. Pittau, Phys. Lett. B **386**, 397 (1996).
[10] T. Stelzer, Z. Sullivan, and S. Willenbrock, Phys. Rev. D **56**, 5919 (1997).
[11] B. W. Harris, E. Laenen, L. Phaf, Z. Sullivan, and S. Weinzierl, Phys. Rev. D **66**, 054024 (2002).
[12] Z. Sullivan, Phys. Rev. D **70**, 114012 (2004).
[13] Q.-H. Cao, R. Schwienhorst, J. A. Benitez, R. Brock, and C. P. Yuan, Phys. Rev. D **72**, 094027 (2005).
[14] J. M. Campbell, R. K. Ellis, and F. Tramontano, Phys. Rev. D **70**, 094012 (2004).
[15] P. Falgari, P. Mellor, and A. Signer, Phys. Rev. D **82**, 054028 (2010).
[16] R. Schwienhorst, C. P. Yuan, C. Mueller, and Q.-H. Cao, Phys. Rev. D **83**, 034019 (2011).
[17] J. Wang, C. S. Li, H. X. Zhu, and J. J. Zhang, arXiv:1010.4509.
[18] N. Kidonakis, Phys. Rev. D **83**, 091503 (2011).
[19] J. Wang, C. S. Li, and H. X. Zhu, Phys. Rev. D **87**, 034030 (2013).
[20] N. Kidonakis, Phys. Rev. D **93**, 054022 (2016).
[21] S. Frixione, E. Laenen, P. Motylinski, and B. R. Webber, J. High Energy Phys. 03 (2006) 092.
[22] S. Alioli, P. Nason, C. Oleari, and E. Re, J. High Energy Phys. 09 (2009) 111; 02 (2010) 11.

[23] R. Frederix, E. Re, and P. Torrielli, J. High Energy Phys. 09 (2012) 130.

[24] M. Brucherseifer, F. Caola, and K. Melnikov, Phys. Lett. B **736**, 58 (2014).

[25] ATLAS Collaboration, Report No. ATLAS-CONF-2014-007, 2014.

[26] CMS Collaboration, Report No. CMS-PAS-TOP-15-007, 2015.

[27] P. Falgari, F. Giannuzzi, P. Mellor, and A. Signer, Phys. Rev. D **83**, 094013 (2011).

[28] A. S. Papanastasiou, R. Frederix, S. Frixione, V. Hirschi, and F. Maltoni, Phys. Lett. B **726**, 223 (2013).

[29] T. Han, G. Valencia, and S. Willenbrock, Phys. Rev. Lett. **69**, 3274 (1992).

[30] M. Assadsolimani, P. Kant, B. Tausk, and P. Uwer, Phys. Rev. D **90**, 114024 (2014).

[31] P. Bolzoni, F. Maltoni, S.-O. Moch, and M. Zaro, Phys. Rev. Lett. **105**, 011801 (2010).

[32] M. Cacciari, F. A. Dreyer, A. Karlberg, G. P. Salam, and G. Zanderighi, Phys. Rev. Lett. **115**, 082002 (2015).

[33] I. W. Stewart, F. J. Tackmann, and W. J. Waalewijn, Phys. Rev. Lett. **105**, 092002 (2010).

[34] R. Boughezal, C. Focke, X. Liu, and F. Petriello, Phys. Rev. Lett. **115**, 062002 (2015).

[35] J. Gaunt, M. Stahlhofen, F. J. Tackmann, and J. R. Walsh, J. High Energy Phys. 09 (2015) 058.

[36] E. L. Berger, J. Gao, C. S. Li, Z. L. Liu, and H. X. Zhu, Phys. Rev. Lett. **116**, 212002 (2016).

[37] W. L. van Neerven and E. B. Zijlstra, Phys. Lett. B **272**, 127 (1991).

[38] E. B. Zijlstra and W. L. van Neerven, Nucl. Phys. **B383**, 525 (1992).

[39] E. B. Zijlstra and W. L. van Neerven, Phys. Lett. B **297**, 377 (1992).

[40] W. L. van Neerven and A. Vogt, Nucl. Phys. **B568**, 263 (2000).

[41] W. L. van Neerven and A. Vogt, Nucl. Phys. **B588**, 345 (2000).

[42] T. Gehrmann and E. W. N. Glover, Phys. Lett. B **676**, 146 (2009).

[43] G. Cullen et al., Eur. Phys. J. C **74**, 3001 (2014).

[44] J. Gao, C. S. Li, and H. X. Zhu, Phys. Rev. Lett. **110**, 042001 (2013).

[45] W. Bernreuther, A. Brandenburg, Z. G. Si, and P. Uwer, Nucl. Phys. **B690**, 81 (2004).

[46] K. Melnikov and M. Schulze, J. High Energy Phys. 08 (2009) 049.

[47] A. Broggio, A. S. Papanastasiou, and A. Signer, J. High Energy Phys. 10 (2014) 098.

[48] S. Dulat, T.-J. Hou, J. Gao, M. Guzzi, J. Huston, P. Nadolsky, J. Pumplin, C. Schmidt, D. Stump, and C. P. Yuan, Phys. Rev. D **93**, 033006 (2016).

[49] M. Cacciari, G. P. Salam, and G. Soyez, J. High Energy Phys. 04 (2008) 063.

[50] We define a parton-level *b* jet as a clustered jet with a nonzero bottom quark number, e.g., a jet containing both a *b* quark and anti-*b* quark is not considered as a *b* jet.

[51] A. Banfi, G. P. Salam, and G. Zanderighi, Eur. Phys. J. C **47**, 113 (2006).

[52] R. Aaij et al. (LHCb Collaboration), J. High Energy Phys. 06 (2012) 058.

[53] CMS Collaboration, Phys. Rev. D **90**, 032004 (2014).

[54] ATLAS Collaboration, Phys. Rev. D **85**, 072004 (2012).

[55] E. L. Berger, F. Halzen, C. S. Kim, and S. Willenbrock, Phys. Rev. D **40**, 83 (1989); **40**, 3789(E) (1989).

[56] L. A. Harland-Lang, A. D. Martin, P. Motylinski, and R. S. Thorne, Eur. Phys. J. C **75**, 204 (2015).

[57] R. D. Ball et al. (NNPDF Collaboration), J. High Energy Phys. 04 (2015) 040.

[58] S. Alekhin, J. Blumlein, and S. Moch, Phys. Rev. D **89**, 054028 (2014).

[59] S. Alekhin, J. Bluemlein, S. Moch, and R. Placakyte, arXiv:1508.07923.

[60] J. Gao, C. S. Li, L. L. Yang, and H. Zhang, Phys. Rev. Lett. **107**, 092002 (2011).